

Article

# On-Board Correction of Systematic Odometry Errors in Differential Robots

S. Maldonado-Bascón<sup>1,†</sup>, R. J. López-Sastre<sup>1,†</sup>, F.J. Acevedo-Rodríguez<sup>1,†</sup> and P. Gil-Jiménez<sup>1,†</sup><sup>1</sup> Dpto. de Teoría de la Señal y Comunicaciones

Escuela Politecnica Superior

Universidad de Alcalá

Alcalá de Henares (Madrid)

<http://agamenon.tsc.uah.es/Investigacion/gram>

\* Correspondence: e-mail: saturnino.maldonado@uah.es

Version November 8, 2018 submitted to Preprints

**Abstract:** An easier method for the calibration of differential drive robots is presented. Most of the calibration is done on-board and it is not necessary to expend too much time taking note of the robot's position. The calibration method does not need a big free space to perform the tests. The bigger space is just in a straight line, which is easy to find. Results with the proposed method are compared with those from UMB as a reference, and they show very little deviation while the proposed calibration is much simpler.

**Keywords:** differential drive robot; calibration; systematic error.

## 1. Introduction

Odometry based on encoder information is the way used to get the relative position on most of the differential drive robots. In this paper, we describe our solution for the calibration of such robots in order to avoid systematic error.

### 1.1. Odometry calculations

As a summary, we include the odometry expressions for differential robots, in order to point out the dependency of those calculations on the parameters we need to calibrate. Iteratively, the position of the robot is obtained by approximation. For a given iteration,  $P_R$  and  $P_L$  represents the pulses of the right and left encoder respectively.

The factor that converts the pulses into mm of linear displacement is  $C_m$ , given by

$$C_m = \frac{\pi D}{C_e}$$

where  $D$  is the wheel diameter and  $C_e$  is the number of pulses per revolution of our encoder. So, in each iteration  $i$ , the distance travelled by the right and left wheels  $\Delta U_{R/L,i}$  is

$$\Delta U_{R/L,i} = C_m P_{R/L,i}$$

The distance travelled by the centre of the wheel axis and the change in the orientation in each iteration are given by

$$\Delta U_i = \frac{1}{2}(\Delta U_{R,i} + \Delta U_{L,i})$$

$$\Delta \theta_i = \frac{1}{b}(\Delta U_{R,i} - \Delta U_{L,i})$$

where  $b$  is the wheelbase: the distance from the contact point of both wheels with the floor. The global orientation is

$$\theta_i = \theta_{i-1} + \Delta \theta_i$$

And finally, the estimated position of the robot for iteration  $i$  is

$$X_i = X_{i-1} + \Delta U_i \cos(\theta_i)$$

$$Y_i = Y_{i-1} + \Delta U_i \sin(\theta_i)$$

17 As can be seen from these equations, they depend on  $D$  and  $b$ , where  $D$  will be  $D_R$  and  $D_L$  because of  
18 the two wheels.

### 19 1.2. Related work

20 Deviations in these parameters produce systematic errors, and a calibration process is necessary  
21 for differential drive robots due to construction errors. Non-systematic errors will appear due to a  
22 slippery or unregular floor, but these are not our objective in this paper.

23 [1] and [2] are the main references for systematic odometry error correction. In [1] a 4 m side square  
24 is travelled clockwise and counterclockwise in order to correct the relation of the wheel diameters and  
25 the distance between the wheels.

There are 3 sources of error. First, in the average wheel diameter  $D_{avg}$ , we consider a scaling factor  $E_s$  from the nominal value.

$$D_{avg} = E_s D_{nom}$$

Second, the fact that the wheel diameters are unequal. Depending on the construction of the wheel, this error can be larger or smaller. If we take the diameter  $D_R$  of the right wheel as a reference, the left diameter  $D_L$  is given by the factor  $E_d$ :

$$D_L = E_d D_R$$

The last error source to adjust is the wheelbase,  $b$ , so the relation between the actual wheelbase,  $b_{act}$  and the nominal is

$$b_{act} = E_b b_{nom}$$

26 Some papers have proposed correcting  $E_d$  and  $E_b$  [1] and [3]. For example, in [4], the 3 parameters are  
27 adjusted.

28 In [4], two experiments are proposed. A movement forward with a rotation of  $\pi$  and then coming  
29 back, one with a clockwise rotation and one counterclockwise. Simulation results are shown, but it  
30 does not indicate the number of iterations of the experiments. In [1], travelling over a 4 m side square  
31 both counterclockwise and clockwise is proposed, 5 times each. One of the problems is that you need  
32 a free space of 4 m  $\times$  4 m plus the dimensions of the robot with a regular non-slippery floor. They  
33 also assumed  $E_s = 1$ , so you need to calibrate  $D_{avg}$  before starting the experiments. The robot must be  
34 placed carefully in the same position and orientation for the 10 trials. In [5], the expressions from [1] are  
35 corrected. They also analyse the effect of the square path size: 1 m  $\times$  1 m was not successful, because  
36 it was too small. Their expressions show in simulation better convergence if the experiment is iterated  
37 and better results for 2 m  $\times$  2 m. In [3] a bidirectional circular path test is proposed to estimate the  
38 correction factors. They said: 'the low noise procedure allows to obtain good results without the need  
39 to repeat the experiments.' They point out that a circular path of 5 m in diameter, that it is even worse  
40 than the 4 m square recommended in [1].

41 A description of self-calibration is presented in [6]. It is based on a laser range finder that allows  
42 high accuracy measurement. Similar papers using laser range finders can be found in the literature,  
43 but those are not related with the present paper.

44 We are looking for a method for occasional calibration that will require little time. Calibration  
45 is important to increase accuracy and to reduce the number of corrections needed using absolute  
46 position estimation: these can be reduced if the relative position is accurate. In the present paper, a  
47 calibration method to reduce systematic relative position error for a differential drive mobile robot  
48 is presented. The proposed method needs just enough space for the robot to turn and to perform a

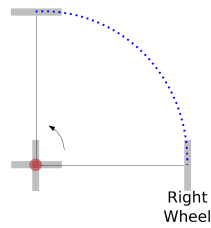


Figure 1. Robot scheme while turning with left wheel stopped.

49 3 m long straight movement. It is also important to note that most of the data for the calibration are  
 50 obtained and calculated on-board. It is not necessary to be careful with the initial position of the robot.  
 51 Both features allow calibrating the robot very quickly.

52 Our research group has been working on developing many different technical aids under the  
 53 solidarity program “Padrino Tecnológico” (<http://padrinotecnologico.org/>), from walkers to electric  
 54 wheelchairs. This is an approach to use robots for assistive tasks. Orientation for people with cognitive  
 55 disorder is being stressed, and helping to increase their autonomy is the first goal of this project,  
 56 although many other functionalities can be included using the same hardware. This is the second  
 57 platform we have worked on. The previous one was too small to get into disabled attention centres.

## 58 2. Calibration method

### 59 2.1. Estimation of $E_d$

The proposed calibration method aims at reducing the time required to perform a calibration. We  
 are searching for the actual  $D_R$ ,  $D_L$  and  $b$ . The first experiment looks for the relation  $E_d = D_R/D_L$ : the  
 robot will describe a circular path with the left wheel stopped for  $N$  rounds. Then, this is repeated with  
 the right wheel stopped for another  $N$  rounds. Fig. 1 represents the robot while turning with a stopped  
 left wheel. The distance travelled,  $s$ , in each round, can be expressed in different ways depending on  
 the **effective** wheelbase, and the number of pulses in each round  $P_{1R}$  and  $P_{1L}$ :

$$s = 2\pi b = \frac{P_{1R}\pi D_R}{c_e} = \frac{P_{1L}\pi D_L}{c_e} \quad (1)$$

60 where  $c_e$  pulses/rev is a constant to translate wheel turns to pulses.

Using Equation (1) yields

$$E_d = \frac{D_L}{D_R} = \frac{P_{1R}}{P_{1L}}$$

61 The movements involved in this test suffer from one problem: stopped wheels need low friction  
 62 to perform the circular movement of the robot but enough friction to get the wheel at the same point.  
 63 When the test is done on a slippery floor, a small piece (see Fig. 2) has been designed to achieve this  
 64 goal, so now the wheel pivots on that piece over an axial bearing. Fig. 3 illustrate the situation of the  
 65 wheel during the test: the wheel, the piece, and the axial bearing are visible.

66 In our case, this modification of the robot structure introduces a little distortion in the mechanism  
 67 system, increasing the height of the stopped wheels by 6 mm, that is, approximately  $0.6^\circ$  for the wheel  
 68 axis. We used the piece on a polished stone floor and we removed it for the lab floor.

69 If a distance or orientation sensor is available, the  $N$  rounds can be monitored in order to extract  
 70 the relation  $E_d$ . In our case, an ultrasound sensor (HC-2R04) has been used to get the distances to the  
 71 obstacles while turning. Fig. 6 and the zoomed Fig. 7 show the distances from the sensor as a function  
 72 of the pulses of the encoder of the moving wheel.

73 The autocorrelation of the sequence of the distances has been obtained and the period  $P_{1R/L}$  can  
 74 be easily extracted onboard if the robot has sufficient capabilities. Fig. 8 shows the autocorrelation for

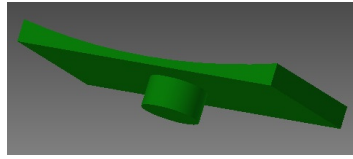


Figure 2. Bearing Base.



Figure 3. Wheel Detail.

75 the distances read from the ultrasound sensor. It must be take into account that these do not necessarily  
 76 have to be accurate distances and the scenario must not be 'periodic', i.e. an irregular one is better in  
 77 order to obtain the number of pulses per turn.

## 78 2.2. Estimation of $D_R$

79 The movement of the robot while trying to travel in a straight line is illustrated in Fig. 4. The  
 80 actual distance from A to B is not the output of the encoder corrected by the conversion factor  $c_m$ .  
 81 However, if the robot's orientation is kept below a given threshold, the maximum deviation of that  
 82 measurement can be controlled. For example, if the orientation remains below  $1^\circ$ , then the maximum  
 83 deviation remains less than 0.02%, and for  $2^\circ$ , less than 0.06%. Those deviations can be accepted for  
 84 our experiments and we will analyse the robot's orientation to reject those measurements where the  
 85 maximum deviation of orientation has been greater than a given threshold.

The right wheel is taken as a reference, and  $D_L$  is corrected by the factor  $E_d$ . In the second  
 experiment, a straight motion for 3 m is performed by the robot, and the number of pulses of the right  
 wheel,  $P_{2R}$ , with the actual distance traveled  $d_{3m}$  gives the conversion factor from pulses to mm as

$$c_m = \frac{d_{3m}}{P_{2R}}$$

The actual  $D_R$  is given by

$$D_R = \frac{c_m c_e}{\pi} \quad (2)$$

86 in our case,  $c_e = 152.7$  pulses/rev.

Coming back to Equation (1), the actual  $b$  is given by

$$b_{act} = \frac{P_{1R} D_R}{2c_e}$$

and  $E_s$  is obtained as the mean of  $D_R$  and  $D_L$ :

$$E_s = \frac{D_R}{D_{nom}} \frac{1 + E_d}{2} \quad (3)$$

87 We found a problem with the effective wheelbase ( $b_{eff}$ ). It is larger when the speed-wheel relation  
 88 is close to unity, and is smaller when one of the wheels is stopped. Most of the movements during

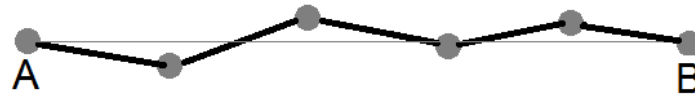


Figure 4. Movement diagram.



Figure 5. Robotic platform.

89 the robot's operation are performed with the two wheels having similar speeds, but the proposed  
90 calibration method uses part of the experiments with one wheel stopped.

In order to get  $b_{eff}$ , we performed a movement turning over one stopped wheel and then turning with both wheels at the same speed, taking into account the number of pulses to complete a turn with the stopped wheel  $P_{0_{R_b}}$  and the number of pulses when turning with the two wheels at the same speed  $P_{0_{R_b/2}}$ . Then, the factor to obtain  $b_{eff}$  is

$$K = \frac{2 * P_{0_{R_b/2}}}{P_{0_{R_b}}}$$

### 91 3. Experiments

Our robot software has 3 parameters to adjust. They are set before starting each calibration method:

$$c_m = \frac{\pi D_{nom}}{c_e} = \frac{\pi 190}{157.2} = 3.80 \text{ mm/pulse}$$

$$E_d = 1$$

and

$$b = 590 \text{ mm}$$

#### 92 3.1. UAH Calibration 1

The first experiment was carried out with the robot platform shown in Fig. 5. First, we obtained the effective wheelbase factor for movements with a stopped wheel, so the robot performed movements as was explained previously. We get  $P_{0_{R_b}} = 951$  pulses and  $P_{0_{R_b/2}} = 478$  pulses, so

$$K = 1.0053.$$

93 Then, with the left wheel stopped, the robot performed a given number of rounds and the  
94 experiment was then repeated for a stopped right wheel.

95 Fig. 6 shows the output of the ultrasound sensor for 7 turns and in Fig. 7 just 2 periods are plotted.  
96 It is important to be sure that the scenario is not symmetrical in order to get the proper period. In  
97 our case, because of the limited sensor range, the scenario must not be very large. Fig. 8 shows the

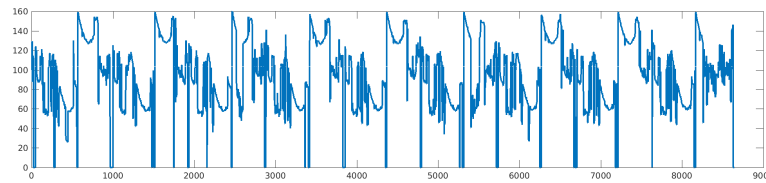


**Figure 6.** Sensor Output rotating over the left wheel.

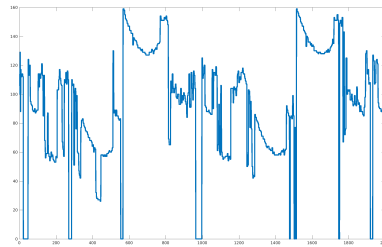


**Figure 7.** Zoom Sensor Output over the left wheel.

**Table 1.** Results from the second experiments

Iteration	$P_{2R}$ (Pulses)	distance (mm)	$max(\theta)$ (degrees)	$c_m$ (mm/pulse)
1	795	3078	0.75	3.87
2	795	3068	0.93	3.86
3	795	3068	0.75	3.86
4	795	3070	0.76	3.86

98 autocorrelation sequence of the sensor output and from this data the period, i.e. the number of pulses  
99 per turn, can be easily obtained.

The number of pulses when the left wheel is stopped per turn (period)  $P_{1R}$  is

$$P_{1R} = \{951.1, 952.0, 951.0\} \text{ pulses}$$

for three iterations, as can be seen the variance for different iterations is low. When the right wheel is stopped,  $P_{1L}$  is

$$P_{1L} = \{944.0, 943.0, 943.0\} \text{ pulses}$$

also for three iterations of the experiment. So, taking the mean value

$$E_d = \frac{D_L}{D_R} = \frac{P_{1R}}{P_{1L}} = 1.007$$

100 Now, in order to perform the second experiment, the  $E_d$  factor must be included in the robot's  
101 odometry, so we set up the new  $E_d$  in the robot software or automatically update it if the calculation is  
102 done on-board.

103 Then a 3m long motion is performed and the number of pulses in several iterations are illustrated  
104 in Table 1, where the number of pulses for the distance actually travelled gives the factor  $c_m$ . The  
105 maximum deviation in orientation is also considered in order to discard those results with deviations  
106 bigger than  $1^\circ$ .

107 From the results in Table 1 we get  $c_m = 3.86$  mm/pulse.

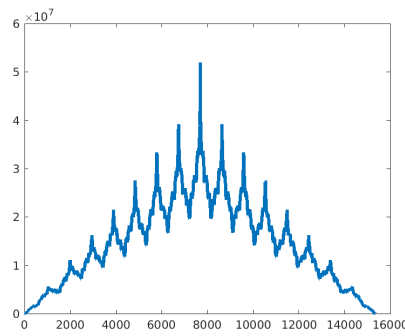


Figure 8. Sensor output autocorrelation sequence.

The wheelbase distance  $b$  can be obtained from

$$2\pi b = P_{1R} \cdot c_m$$

but  $P_{1R}$  was obtained from a movement with stopped left wheel, so it must be corrected with  $K$ :

$$2\pi \frac{b}{K} = P_{1R} \cdot c_m$$

108 so,  $b = \frac{951.3 \cdot 3.86 \cdot 1.0053}{2\pi} = 586.5$  mm, from Equation (2)  $D_R = 187.61$  mm and from Equation (3)  
 109  $E_s = 0.9924$  where the used nominal diameter was  $D_{nom} = 190$  mm and the new average of the  
 110 diameters is  $D_{avg} = 188.55$  mm. We do not use  $D_{avg}$  but it will be necessary to perform a calibration  
 111 from [1] for comparison.

### 112 3.2. UMB Calibration

The  $D_{avg}$  from UAH calibration 1 is used to perform the UBM calibration [1]. The setup parameters are

$$c_m = \frac{\pi D_{nom}}{c_e} = \frac{\pi 188.55}{152.7} = 3.88$$

$$E_d = 1$$

and

$$b = 590.$$

113 The UMB method [1] was carried out for a square of  $L = 2$  m (as was suggested in [5]) for 5  
 114 rounds clockwise and 5 counterclockwise, writing the final point deviations of each movement. Our  
 115 robot platform is almost 1 m long and a larger free scenario was not viable.

The results for the error centres of gravity for clockwise ( $X_{cg,cw}$ ,  $Y_{cg,cw}$ ) and counterclockwise ( $X_{cg,ccw}$ ,  $Y_{cg,ccw}$ ) are

$$X_{cg,cv/ccw} = \frac{1}{5} \sum_{i=1}^5 \epsilon_{x_{i,cv/ccw}}$$

$$Y_{cg,ccw} = \frac{1}{5} \sum_{i=1}^5 \epsilon_{y_{i,cv/ccw}}$$

where the error is the difference between the actual absolute position of the robot and the calculated one.

$$\epsilon_x = x_{abs} - x_{calc}$$

$$\epsilon_y = y_{abs} - y_{calc}$$

**Table 2.** Validation Results 3m

Method	$\epsilon_x$ (mm)
Before cal.	80
Before cal.	80
Before cal.	83
UAH	16
UAH	23
UAH	7
UMB	-4
UMB	-8
UMB	-5

$$\begin{aligned} X_{cg,ccw} &= 24.0 & Y_{cg,ccw} &= -34.6 \\ X_{cg,cw} &= -65.6 & Y_{cg,cw} &= 53.0 \end{aligned}$$

Using the equations from [1]:

$$\alpha = \frac{X_{cg,cw} + X_{cg,ccw}}{-4L} \frac{180^\circ}{\pi}$$

in degrees, the previous results give  $\alpha = 0.298$  and

$$\beta = \frac{X_{cg,cw} - X_{cg,ccw}}{-4L} \frac{180^\circ}{\pi}$$

in degrees,  $\beta = 0.642$ , so:  $b_{actual} = 591.96$  mm and  $E_d = 1.003$ .

If the correction from [5] is included, a slight change is obtained:  $b_{actual} = 591.98$  mm.

#### 4. Validation

In [1], the same experiment used for calibration is repeated after calibration in order to test the method. The distances from zero error to the centres of gravity are used to compare the results. This validation process needs a large space to perform the test. In [4] and [3], only simulation results are presented to compare the methods.

Table 2 shows the error in the first 3 m of the experiment, and Table 3 the error after the whole journey.

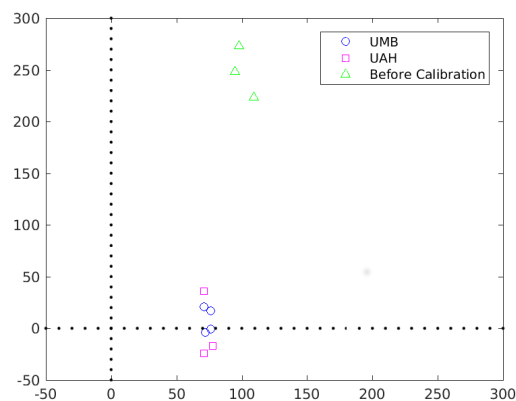
To validate the results of calibration, travelling along a 3 m long path, followed by a turn through an angle of  $\pi$  and then coming back again 3 m, was carried out. Table 2 and 3 show the error ( $\epsilon_x = x_{abs} - x_{calc}$  and  $\epsilon_y = y_{abs} - y_{calc}$ ) in mm in the X and Y coordinates before calibration for the calibration method UAH and for UMBmark. Table 2 after the first 3 m of travel and Table 3 after coming back.

The tests were been performed 3 times for each calibration in order to avoid non-systematic error. Note that the error in Table 2 comes basically from the error in the wheel diameters and the error in Table 3 is affected by the wheel diameters and  $b$ .

Fig. 9 shows the error before calibration, with the UMB method calibration and the proposed one. As can be seen, the results for both calibrations are very similar, although slightly better for the UMB method. But the simplicity of our method leads us to use it instead of the UMB. It must be taken into account that most of the measurements in the proposed method are done on-board and in most of the movements, the initial point is not important.

**Table 3.** Validation Results 3m- $\pi$ -3m

Method	$\epsilon_x$ (mm)	$\epsilon_y$ (mm)
Before cal.	109	223
Before cal.	98	273
Before cal.	95	248
UAH 1	71	36
UAH 1	78	-17
UAH 1	71	-24
UMB	72	-4
UMB	71	21
UMB	76	17

**Figure 9.** Error from different calibrations.

## 139 5. Conclusions

140 A new method for differential drive robot calibration has been presented. One of the main  
 141 contributions is that free space needed to perform the calibration in our method is very small. Another  
 142 feature to point out is that the number of manual measurements is just one with our method, which  
 143 can be repeated in order to check the correctness, but checking the maximum orientation makes it easy  
 144 to discard wrong measurements. The most complicated part of the calibration method can be done  
 145 on-board. If a calibrated distance sensor is available, the whole method can be implemented on-board.

146 The results are very close to those obtained with the UMB method, so we use our method instead  
 147 because of its simplicity in performing the calibration.

148 **Funding:** This work was partially supported by the University Alcala research program through the projects  
 149 CCG2016/EXP-045 and CCG2016/EXP-042 and TEC2016-80326-R from the “Ministerio de Economía, Industria y  
 150 Competitividad”.

151 **Author Contributions:** All authors contributed equally to this work.

152 **Conflicts of Interest:** The authors declare that there are no conflicts of interest regarding the publication of this  
 153 paper.

## 154 References

- 155 1. J. Borenstein and L. Feng, “Correction of systematic odometry errors in mobile robots,” in *Intelligent Robots*  
 156 *and Systems 95. Human Robot Interaction and Cooperative Robots*, Proceedings. 1995 IEEE/RSJ International  
 157 Conference on, vol. 3. IEEE, 1995, pp. 569–574.

- 158 2. ———, "Measurement and correction of systematic odometry errors in mobile robots," *IEEE Transactions on*  
159 *robotics and automation*, vol. 12, no. 6, pp. 869–880, 1996.
- 160 3. T. Abbas, M. Arif, and W. Ahmed, "Measurement and correction of systematic odometry errors caused by  
161 kinematics imperfections in mobile robots," in *SICE-ICASE, 2006. International Joint Conference*. IEEE, 2006,  
162 pp. 2073–2078.
- 163 4. A. Bostani, A. Vakili, and T. A. Denidni, "A novel method to measure and correct the odometry errors in  
164 mobile robots," in *Electrical and Computer Engineering, 2008. CCECE 2008. Canadian Conference on*. IEEE,  
165 2008, pp. 000 897–000 900.
- 166 5. K. Lee, C. Jung, and W. Chung, "Accurate calibration of kinematic parameters for two wheel differential  
167 mobile robots," *Journal of mechanical science and technology*, vol. 25, no. 6, p. 1603, 2011.
- 168 6. A. Martinelli, N. Tomatis, and R. Siegwart, "Simultaneous localization and odometry self calibration for  
169 mobile robot," *Autonomous Robots*, vol. 22, no. 1, pp. 75–85, 2007.